Rigid-Ruling Folding Compatibility of Planar Creases

K. Mundilova, G. Nawratil

Abstract: *Planar curved creases represent an important family of creases and offer significant potential for application in interactive design tools. Once a folded state is constructed, the question arises: Does a folding motion exist, maintaining the same ruling layout, that connects the flat state to the folded state? This is referred to as a rigid-ruling folding motion.*

In this paper, we characterize combinations of planar curves that allow a rigid-ruling folding motion and illustrate our theoretical findings with examples.

1 Introduction

Deployable structures transition from compact to expanded forms, mirroring nature's mechanisms like insect wings and flower petals. Their efficiency and functionality are used in applications such as in space engineering, medical surgical items, and everyday items like umbrellas. With advancements in computational technology, the study of deployable structures has become a dynamic area of research. However, despite the increasing potential of computational methods, analyzing and designing these systems remains a complex task.

Inspired by architectural applications, recent work has also considered semi-discrete structures, which are composed of strips of developable surfaces [Liu et al. 06]. Such surfaces can be flattened into the plane without stretching or tearing and are known to carry a family of lines, the so-called *rulings*. When considering the bending of such developable surfaces, each ruling acts as a hinge. In the literature, such a motion for an individual developable strip is called a *rigid-ruling folding motion* [Demaine et al. 15, Mundilova 23] or *isometric deformation* [Nawratil 23].

A particularly interesting special case of semi-discrete structures made from developable strips is *curved-crease folding*, where the strips fit together in their developed state and can thus be created by creasing flat material along curves. Due to their aesthetic appeal and straightforward fabrication, curved-crease origami has found many artistic explorations such as in the works of David Huffman [Demaine et al. 11, Koschitz 14]. Previous work demonstrates that combinations of *tangent-parallel curves*, that is, curves whose tangents at points connected by a ruling are parallel, allow a rigid-ruling folding motion [Tachi 11, Mundilova 23]. Another

Figure 1: *Construction of planar curved creases by splitting the surface with a plane and reflecting one part onto the other side.*

family of creases that allow a rigid-ruling folding motion was highlighted by [Demaine et al. 18] in their analysis of combinations of constant fold-angle creases between cylinders and cones.

Beyond constant fold-angle creases, planar creases represent another significant category. Given a developable surface, planar creases can be easily created by splitting the surface with an appropriate plane into two connected subpatches and then mirroring one of the subpatches onto the plane, as illustrated in Figure 1. Due to this simple construction, this method offers numerous possibilities for use in interactive design tools [Mitani and Igarashi 11, Mitani 12, Mundilova et al. 23].

In this paper, we explore combinations of planar creases that allow a rigid-ruling folding motion, which can be reduced[1] to analyzing isometric deformations of cones and cylinders that maintain the planarity of two curves. The discrete case has been recently completely characterized by [Nawratil 23]. Additionally, Nawratil provides an analysis of the smooth cylindrical case, though his investigation into cones remains incomplete.

Our contribution finalizes the discussion of the conical case by showing that the only compatible curves are tangent-parallel; i.e. located in parallel planes. Consequently, this also provides a complete classification of planar creases compatible with rigid-ruling folding motions.

The structure of this paper is organized as follows: Section 2 reviews the theoretical background and essential definitions. Section 3 examines isometric deformations of developable surfaces, specifically focusing on the case where the planarity of a specific curve is preserved. Section 4 introduces the main result of this paper concerning the compatibility of planar curves under isometric deformations. The paper concludes by applying the theory to origami shapes and analyzing the feasibility of rigid-ruling folding motions in Section 5. Finally, it should be noted that all proofs are given in the appendix in order to streamline the paper.

2 Notation and Properties of Developable Surfaces

In this section, we establish the foundation of our analysis of developable surfaces, which we parametrize as ruled surfaces while imposing an additional constraint

[1] According to [Sauer 70] the deformation of tangent developable surfaces can be reduced to cones.

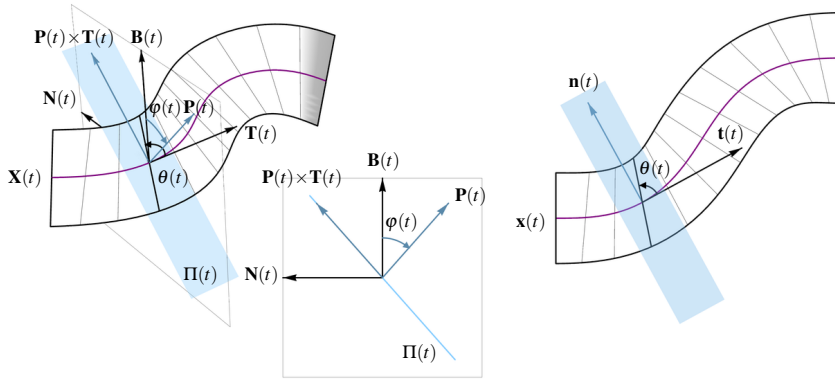

Figure 2: *Illustration of the notation introduced in Section 2.*

to ensure developability. We follow the notation used by [Mundilova 23], which builds upon works of [Demaine et al. 15, Demaine et al. 18].

2.1 Ruled Surfaces

In the following, we parametrize a *ruled surface* as

$$\mathbf{S}(t,u) = \mathbf{X}(t) + u\mathbf{R}(t), \tag{1}$$

where $\mathbf{X}(t) : T \to \mathbb{R}^3$ is a curve, the *directrix*, and $\mathbf{R}(t) : T \to S^2$ are unit-length vectors, the so-called *ruling directions*. Without loss of generality, we assume $T = [0, t_{\max}]$, for some $t_{\max} > 0$, and $u \in \mathbb{R}$. Additionally, for the surface to be C^2, we require both $\mathbf{X}(t)$ and $\mathbf{R}(t)$ to be C^2.

We assume that the curve is equipped with an orthonormal frame and we describe the location of the ruling vectors with respect to this frame. To ensure that the curve's frame is continuous, we define the curve $\mathbf{X}(t)$ through three functions: $K(t) : T \to \mathbb{R}$, $\tau(t) : T \to \mathbb{R}$, and $s(t) : T \to \mathbb{R}$ which define $\mathbf{X}(t)$ up to Euclidean motion through the Frenet-Serret formulas, that is, $\mathbf{X}'(t) = s'(t)\mathbf{T}(t)$, where

$$\begin{pmatrix} \mathbf{T}'(t) \\ \mathbf{N}'(t) \\ \mathbf{B}'(t) \end{pmatrix} = s'(t) \begin{pmatrix} 0 & K(t) & 0 \\ -K(t) & 0 & \tau(t) \\ 0 & -\tau(t) & 0 \end{pmatrix} \begin{pmatrix} \mathbf{T}(t) \\ \mathbf{N}(t) \\ \mathbf{B}(t) \end{pmatrix}. \tag{2}$$

Here we require that the $K(t)$, $\tau(t)$, and $s'(t)$ are continuous, and $s'(t) > 0$.

Note that we allow $K(t)$ to take negative values. Moreover, isolated points or intervals where $K(t) = 0$ or $\tau(t) = 0$ still yield a continuous frame $(\mathbf{T}(t), \mathbf{N}(t), \mathbf{B}(t))$. The described frame is not a Frenet-frame. However, at parameter values where the Frenet-frame is defined, the computed frame coincides with the Frenet-frame, differing only by sign. Moreover, $K(t)$ corresponds to the curvature of the directrix up to sign, while $\tau(t)$ is the torsion of the directrix when defined. In the following,

we refer to $K(t)$ as the *(signed) curvature* and to $\tau(t)$ as the *torsion*. Furthermore, $s(t)$ denotes the *arc-length* of the directrix, and $s'(t)$ represents the *parametrization speed*.

To determine the ruling directions with respect to the frame $(\mathbf{T}(t),\mathbf{N}(t),\mathbf{B}(t))$, we introduce two additional angular functions: the *inclination angle* $\varphi(t) : T \to \mathbb{R}$ and the *ruling angle* $\theta(t) : T \to \mathbb{R}$; see Figure 2.

The inclination angle $\varphi(t)$ encodes the angle between a one-parameter family of planes $\Pi(t)$, which contain the curve's tangent vectors $\mathbf{T}(t)$. Those planes will correspond to the tangent planes if the ruled surface is developable. We express the normal vector $\mathbf{P}(t)$ of $\Pi(t)$ as

$$\mathbf{P}(t) = \cos\varphi(t)\ \mathbf{B}(t) + \sin\varphi(t)\ \mathbf{N}(t), \tag{3}$$

resulting in $\varphi(t)$ being the signed angle between $\mathbf{P}(t)$ and $\mathbf{B}(t)$.

Within the plane $\Pi(t)$, we locate the ruling direction using the ruling angle as

$$\begin{aligned}\mathbf{R}(t) &= \cos\theta(t)\ \mathbf{T}(t) + \sin\theta(t)\,(\mathbf{P}(t)\times\mathbf{T}(t)) \\ &= \cos\theta(t)\ \mathbf{T}(t) + \sin\theta(t)\,(\cos\varphi(t)\ \mathbf{N}(t) - \sin\varphi(t)\ \mathbf{B}(t))\,.\end{aligned} \tag{4}$$

For the ruling direction to be C^2, we require both $\theta(t)$ and $\varphi(t)$ to be C^2. Note that for the subsequent computations, C^1 would be sufficient. However, to use known properties of smooth developable surfaces we make this stronger smoothness assumption.

2.2 Developable Surfaces

It is known that the ruled surface in Equation (1) is developable if for all rulings, the tangent planes along points on a ruling are the same [Pottmann and Wallner 10]. This condition can be expressed as

$$\det\left(\mathbf{X}'(t),\mathbf{R}(t),\mathbf{R}'(t)\right) = 0. \tag{5}$$

Using Equation (2) and Equation (4) for ruled surfaces with planar directrices, this condition simplifies to

$$\frac{\varphi'(t)}{s'(t)} = \tau(t) + K(t)\sin\varphi(t)\cot\theta(t); \tag{6}$$

see [Mundilova 23] for more details.

Given a developable surface $\mathbf{S}(t,u)$, we will parametrize its flattened configuration, the *development*, by $\mathbf{s}(t,u) = \mathbf{x}(t) + u\mathbf{r}(t)$, where $\mathbf{x}(t) : T \to \mathbb{R}^2$ represents the 2D counterpart of the directrix $\mathbf{X}(t)$, and $\mathbf{r}(t) : T \to S^1$ the unit-length 2D ruling direction; see Figure 2.

To obtain the developed directrix $\mathbf{x}(t)$, we consider the *geodesic curvature* of $\mathbf{X}(t)$ as a curve on $\mathbf{S}(t,u)$, that is, the curvature of the projection of $\mathbf{X}(t)$ on $\Pi(t)$ at parameter t,

$$k(t) = K(t)\cos\varphi(t). \tag{7}$$

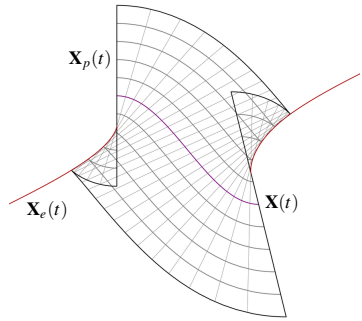

Figure 3: *Developable patch with tangent-parallel curves $\mathbf{X}_p(t)$ (gray) of the directrix $\mathbf{X}(t)$ (purple) and curve of regression $\mathbf{X}_e(t)$ (red).*

We obtain $\mathbf{x}(t)$ by determining the 2D curve with signed curvature $k(t)$ and parametrization speed $s(t)$. This amounts in solving the system of differential equations $\mathbf{x}'(t) = s'(t)\mathbf{t}(t)$, where

$$\begin{pmatrix} \mathbf{t}'(t) \\ \mathbf{n}'(t) \end{pmatrix} = s'(t) \begin{pmatrix} 0 & k(t) \\ -k(t) & 0 \end{pmatrix} \begin{pmatrix} \mathbf{t}(t) \\ \mathbf{n}(t) \end{pmatrix}. \tag{8}$$

As isometry preserves angles on surfaces, particularly the oriented angle between $\mathbf{T}(t)$ and $\mathbf{R}(t)$ or $\mathbf{P}(t) \times \mathbf{T}(t)$, the developed ruling directions read

$$\mathbf{r}(t) = \cos\theta(t)\ \mathbf{t}(t) + \sin\theta(t)\ \mathbf{n}(t).$$

Conversely, when a parametrization of $\mathbf{s}(t,u) = \mathbf{x}(t) + u\mathbf{r}(t)$ is given, the characterizing quantities $s'(t)$, $k(t)$, and $\theta(t)$ can be obtained as follows: First, set $s'(t) = |\mathbf{x}'(t)|$, and define $\mathbf{t}_i(t) = \frac{1}{s_i'(t)}\mathbf{x}_i'(t)$ and $\mathbf{n}_i(t) = \frac{1}{|\mathbf{t}_i'(t)|}\mathbf{t}_i'(t)$. This implies the curvature $k_i(t) = \frac{1}{s_i'(t)}\mathbf{t}_i'(t) \cdot \mathbf{n}_i(t)$ and the ruling directions $\theta_i(t) = \arccos(\mathbf{r}(t) \cdot \mathbf{t}_i(t))$.

2.3 Tangent-parallel Curves

A special class of curves on a developable patch with a specified curve $\mathbf{X}(t)$ are curves whose tangents are parallel at points connected by a ruling, as shown in Figure 3. Such curves essentially copy the kinematic behaviour, and thus they find application in the construction of general rigidly foldable structures, such as [Tachi and Epps 11, Jiang et al. 20, Mundilova 23].

In particular, as the tangents are parallel in 2D, the orthonormal frames are the same. It follows that

$$s_1'(t)k_1(t) = \mathbf{t}_1'(t) \cdot \mathbf{n}_1(t) = \mathbf{t}_2'(t) \cdot \mathbf{n}_2(t) = s_2'(t)k_2(t).$$

Similarly, in 3D, the fact that the orthonormal frames have identical tangent directions implies that their first derivatives, the normals, are identical. Hence, the frames of tangent-parallel curves coincide resulting in

$$s_1'(t)K_1(t) = \mathbf{T}_1'(t) \cdot \mathbf{N}_1(t) = \mathbf{T}_2'(t) \cdot \mathbf{N}_2(t) = s_2'(t)K_2(t).$$

Additionally, $\varphi_1(t) = \varphi_2(t)$, and $\theta_1(t) = \theta_2(t)$. Particularly, if $\mathbf{X}_1(t)$ is planar, and $\mathbf{X}_2(t)$ is tangent-parallel to $\mathbf{X}_1(t)$, it follows that $\mathbf{X}_2(t)$ is planar too.

2.4 Ruling Curvature

In subsequent sections, we will consider isometric deformations $\mathbf{S}(t,u)$ of a specified planar developable patch $\mathbf{s}(t,u)$. To show that two such deformations are identical, we calculate the curvature that indicates the surface's bend perpendicular to the rulings, following the methodology of [Demaine et al. 15,Demaine et al. 18]. This *ruling curvature* is the normal curvature at a given point on an arc-length parametrized curve perpendicular to the rulings at parameter t, expressed as:

$$V(t) = s'(t)K(t)\sin\varphi(t)\frac{1}{\sin\theta(t)}. \tag{9}$$

The ruling curvatures $V_1(t)$ and $V_2(t)$ of two isometric deformations $\mathbf{S}_1(t,u)$ and $\mathbf{S}_2(t,u)$ of the same developed patch with specified rulings are identical, if and only if the deformations are the same (up to Euclidean motion).

3 Isometric Deformations of Developable Surfaces

We now proceed to study configurations of a developable surface with prescribed rulings. Specifically, we examine parametrizations that preserve point-to-point correspondence between the flat and bend states, also known as *isometric deformations*. Recall that two surface parametrizations are considered to be isometric if their first fundamental forms are identical.

First, we will show a useful connection between isometric deformations of tangent developables and cones that share the same ruling directions, which we will refer to as *ruling cones*. Then, we will explore analytic computation of isometric deformations that preserve the planarity of a single curve.

3.1 Linking Isometric Deformations of Tangent Developables and Cones

Given a developable surface, we define its *ruling cone* as the cone with its apex located at the origin and with parallel rulings. In what follows, we demonstrate that for any given curve on a tangent developable patch, we can find a corresponding curve on its ruling cone such that, in all possible configurations of the surface and its associated ruling cone, the corresponding tangents of the curves are parallel. This extends the results presented by [Sauer 70], who explored the relationship between planar curves on configurations of surfaces and their ruling cones. While we mention this generalization, in the proof of the main result in Theorem 1 we will only use the results on planar curves. The proofs of the lemmata presented in this section are provided in Appendix A.

In the following, we consider the parametrization of a planar tangent developable surface, that is, $\mathbf{s}_c(t,u) = \mathbf{c}(t) + u\mathbf{r}(t)$, where $\mathbf{c}(t)$ is the surface's edge of regression, that is, $\mathbf{c}'(t)$ and $\mathbf{r}(t)$ are parallel. Additionally, let $\mathbf{s}_\triangle(t,u) = u\mathbf{r}(t)$ be a parametrization of its ruling cone. First, we show:

Lemma 1. *Up to Euclidean motion, every isometric deformation of $\mathbf{s}_c(t,u)$ corresponds to exactly one isometric deformation of $\mathbf{s}_\triangle(t,u)$ and a C^0 function $s_c'(t) > 0$.*

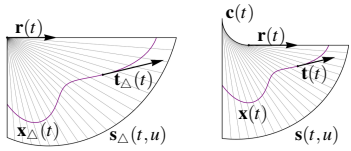

(a) *Planar surface* $\mathbf{s}(t,u)$ *(right) and its ruling cone* $\mathbf{s}_\triangle(t,u)$ *(left) with curves with parallel tangents.*

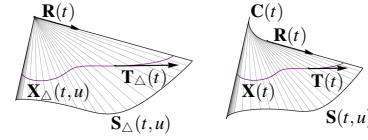

(b) *Corresponding surfaces* $\mathbf{S}(t,u)$ *(right) and ruling cone* $\mathbf{S}_\triangle(t,u)$ *(left) and curves with parallel tangents.*

Figure 4: *Illustration of the notation and concepts presented in Section 3.1.*

Next, we examine a pair of curves on $\mathbf{s}_c(t,u)$ and $\mathbf{s}_\triangle(t,u)$ that have parallel tangents. Specifically, the curve $\mathbf{x}_c(t) = \mathbf{c}(t) + l(t)\mathbf{r}(t)$ on $\mathbf{s}_c(t,u)$ and the curve $\mathbf{x}_\triangle(t) = l_\triangle(t)\mathbf{r}(t)$ on $\mathbf{s}_\triangle(t,u)$ have parallel tangents, if the length functions $l(t)$ and $l_\triangle(t)$ satisfy $|\mathbf{x}_c'(t) \times \mathbf{x}_\triangle'(t))| = 0$. This constraint simplifies to

$$\frac{l_\triangle'(t)}{l_\triangle(t)} = \frac{s_c'(t) + l'(t)}{l(t)} \qquad \Longrightarrow \qquad l_\triangle(t) = l(0)e^{\int_0^t \frac{s_c'(\bar{t}) + l'(\bar{t})}{l(\bar{t})} d\bar{t}}. \tag{10}$$

Lemma 2. *In each pair of isometric deformations,* $\mathbf{S}_c(t,u) = \mathbf{C}(t) + u\mathbf{R}(t)$ *and* $\mathbf{S}_\triangle(t,u) = u\mathbf{R}(t)$*, corresponding to* $\mathbf{s}_c(t,u)$ *and* $\mathbf{s}_\triangle(t,u)$ *respectively, the tangents of the curves* $\mathbf{X}_c(t) = \mathbf{C}(t) + l(t)\mathbf{R}(t)$ *and* $\mathbf{X}_\triangle(t) = l_\triangle(t)\mathbf{R}(t)$ *are parallel.*

3.2 Isometric Deformations that Preserve the Planarity of One Curve

Without limitations, a developable patch possesses an infinite number of degrees of freedom, leading to numerous possible configurations. However, by constraining one curve to be planar, we demonstrate that there exists only a one-parameter family of configurations, as illustrated in Figure 5. Generally, constraining two curves to be planar is over-constraining and can only be satisfied in special cases. The main result of this paper, presented in the next section, classifies combinations of curves that maintain planarity under isometric deformations.

Let $\mathbf{s}(t,u) = \mathbf{x}(t) + u\mathbf{r}(t)$ represent a planar developable surface. Denote the parametrization speed of $\mathbf{x}(t)$ as $s'(t)$, its curvature as $k(t)$, and the ruling angles as $\theta(t)$. In the following, we focus only on the case where the tangents of $\mathbf{x}(t)$ are not parallel to the incident ruling direction, that is, $\mathbf{x}(t)$ does not contain a point of the edge of regression. Specifically, we restrict $\theta(t) \in (0,\pi)$.

We demonstrate that, given a suitable initial value, there exists a unique configuration $\mathbf{S}(t,u) = \mathbf{X}(t) + u\mathbf{R}(t)$ of $\mathbf{s}(t,u)$, up to Euclidean motion, that preserves the planarity of $\mathbf{X}(t)$. In the following, we will show how to compute the curvature $K(t)$ of $\mathbf{X}(t)$ and the inclination angles $\varphi(t)$ of $\mathbf{S}(t,u)$. As the curve $\mathbf{X}(t)$ is planar, its torsion $\tau(t) = 0$.

For the 3D configuration to be isometric to $\mathbf{s}(t,u)$, we require it to be developable, satisfying Equation (6). Consequently, when $\varphi(0) = \varphi_0$, the inclination

(a) *Full motion of a generic example. The isometric deformation is limited by the configuration in which the first tangent plane becomes perpendicular to the base plane.*

(b) *Example with perpendicular rulings* $\left(\theta(t)=\frac{\pi}{2}\right)$. *In this case, the isometric deformation can reach a fully "rolled-up" configuration corresponding to* $\varphi(t)=\pm\frac{\pi}{2}$.

(c) *Example with a straight directrix* $(k(t)=0)$. *In this case, the geometry varies only by the angle between the planar strip and the base plane.*

Figure 5: *Illustration of isometric deformation that preserve the planarity of the one boundary curve.*

angle reads

$$\varphi(t)=\arcsin\left(ce^{I(t)}\right) \qquad \text{where} \qquad I(t)=\int_0^t s'(\tilde{t})k(\tilde{t})\cot\theta(\tilde{t})\,d\tilde{t}, \tag{11}$$

where $c=\sin\varphi_0$. Note that for the solution to be real-valued for all $t\in T$, we require that

$$|c|=|\sin\varphi_0|\leq\min_{t\in T}e^{-I(t)}=c_{\max},$$

where $c_{\max}$ is the absolute value of the sine of the maximal initial inclination angle. Note that this value depends on the interplay between the curve and the ruling direction and can be intuitively interpreted as the value where a tangent plane of the patch becomes perpendicular to the base plane; see Figure 5a.

Upon successful computation of $\varphi(t)$, the curvature follows from Equation (7) as $K(t)=k(t)/\cos\varphi(t)$. Finally, the curve $\mathbf{X}(t)$ and the ruling directions $\mathbf{R}(t)$ follow from Equation (2) and Equation (4), respectively. Note that two configurations that differ only by the sign of c are related by a reflection on the base plane of $\mathbf{X}(t)$. We conclude:

Corollary 1. *Let* $\mathbf{s}(t,u)=\mathbf{x}(t)+u\mathbf{r}(t)$ *be the planar developable surface with prescribed rulings. For all* c *with* $|c|\in[0,c_{\max}]$, *up to Euclidean motion, there exists a unique isometric deformation* $\mathbf{S}(t,u)=\mathbf{X}(t)+u\mathbf{R}(t)$ *of* $\mathbf{s}(t,u)$ *such that* $\mathbf{X}(t)$ *is planar.*

Special cases. Usually, $c_{\max} < 1$ and the isometric deformation exist only for values close to zero. There are, however, two special cases, where the full motion is possible, that is $c_{\max} = 1$:

- If $\theta(t) = \frac{\pi}{2}$, the rulings are perpendicular to the tangents of the directrix. For $c = c_{\max} = 1$, we have $K(t) = \infty$, corresponding to a completely "rolled up" configuration; see Figure 5b.
- If $k(t) = 0$ for all $t \in T$, the curve is a straight line. In this case, the curve remains straight during isometric deformation since $K(t) = 0$. Note that in this case, the surface does not bend and only its position with respect to the base plane changes; see Figure 5c.

4 Main Result

Next, we provide a characterization of curves that remain planar during isometric deformations of developable patches.

Theorem 1. *Consider a planar developable patch with prescribed rulings defined by* $\mathbf{s}(t,u) = \mathbf{x}_1(t) + u\mathbf{r}(t)$ *with* $t \in T$ *and* $u \in \mathbb{R}$*, where the continuous curvature* $k_1(t)$ *of* $\mathbf{x}_1(t)$ *vanishes only at isolated values of* t*. Let* $c_{1,\max} \leq 1$ *be the absolute value of the sine of the maximal initial inclination angle of an isometric deformation* $\mathbf{S}(t,u) = \mathbf{X}_1(t) + u\mathbf{R}(t)$ *of* $\mathbf{s}(t,u)$ *that preserves the planarity of* $\mathbf{X}_1(t)$*.*

For a curvature-continuous curve $\mathbf{x}_2(t)$ *that remains planar during all isometric deformations of* $\mathbf{s}(t,u)$ *preserving the planarity of* $\mathbf{X}_1(t)$ *with* $c_1 \leq c_{1,\max}$*, holds:*

- *If* $|\mathbf{R}'(t)| = 0$ *for all* $t \in T$*, the normals of the base planes of* $\mathbf{X}_1(t)$ *and* $\mathbf{X}_2(t)$*, and the constant ruling direction* $\mathbf{R}(t)$ *are coplanar.*
- *Otherwise, the curve* $\mathbf{x}_2(t)$ *is a tangent-parallel curve of* $\mathbf{x}_1(t)$*.*

Proof overview. On a higher level, in the proof presented in Appendix B, we consider two parametrizations of the developed configuration: $\mathbf{s}_1(t,u) = \mathbf{x}_1(t) + u\mathbf{r}(t)$ and $\mathbf{s}_2(t,u) = \mathbf{x}_2(t) + u\mathbf{r}(t)$, where $\mathbf{x}_1(t)$ and $\mathbf{x}_2(t)$ coincide with the same ruling at parameter t. For both parametrizations, we compute their isometric deformations $\mathbf{S}_i(t,u) = \mathbf{X}_i(t) + u\mathbf{R}(t)$ that preserve the planarity of their respective curves $\mathbf{X}_i(t)$. The overall objective of the proof is to characterize the cases in which the ruling curvatures $V_i(t)$ of $\mathbf{S}_i(t,u)$ are the same, and hence the curves can be positioned on a common isometric deformation of $\mathbf{s}(t,u)$.

This analysis, which is presented in greater detail in the appendix, is conducted through the following four steps:

- *Step 1:* First, we prepare the notation and establish the necessary constraints for the quantities associated with the two patches.
- *Step 2:* Second, we focus on parameter values with non-zero curvature $k_1(t)$ of $\mathbf{x}_1(t)$ and analyze the constraints established in Step 1 for cylinders and cones separately.
- *Step 3:* For both cylinders and cones, we consider combinations of curves with isolated parameter values t^* with vanishing curvature; i.e. $k_1(t^*) = 0$.

- *Step 4:* Finally, we apply the results from Section 3.1 to verify the statement for the remaining case involving general developables.

□

5 Applications

Equipped with the characterization of planar curves that remain planar during isometric deformations, we now apply our findings to establish the (non-)existence of rigid folding motions for some origami shapes using Theorem 1. Additionally, we highlight the implication of our results in the context of semi-discrete T-hedra.

5.1 Origami-shapes that have a Rigid-ruling Folding Motion

The first example of an origami shape exhibiting a rigid-ruling folding motion is David Huffman's wave design, which employs a series of scaled sine curves [Koschitz 14, Figure 4.1.7]; see Figure 6a. Duks Koschitz also reconstructed the rulings from David Huffman's notes and conducted initial numerical experiments. According to the theory presented in this paper, this shape is rigid-ruling foldable. Additionally, since the sine curves remain planar, the profile curves of the folded cylinders are circular arcs.

Another prominent example of a rigid-ruling foldable shape is one half of Ron Resch's design "Yellow Folded Cones: Kissing." [Koschitz 14, Figure 4.2.17]; see Figure 6b. Here, a cone with circular base is equipped with two planar creases that lie in parallel planes.

David Huffman's "Cone reflection parallel to axis" [Koschitz 14, Figure 4.2.48] is obtained by folding a right-rotational cone along parallel planes that are additionally parallel to its axis, resulting in creases that are hyperbolas in the 3D folded state; see Figure 6c. Note that in this case, the crease only locally actuate the isometric deformation and the shape of the full cone is not defined by the creases.

The last example of a rigid-ruling foldable family of shapes are column-shaped origami designs with planar creases [Mitani 12], as the curved crease base planes are coplanar with the rulings of the involved cylinders.

5.2 Origami-shapes that do not have a Rigid-ruling Folding Motion

Next, we turn our attention to two examples of shapes that do not have a rigid-ruling folding motion.

A prominent example obtained by reflecting cones along non-parallel planes is David Huffmans design "Cone, reflected seven times" [Koschitz 14, Figure 4.2.40]; see Figure 6d. Here, a right rotational cone is folded along planes that change their inclination angle with respect to the base of the cone. Similar to before, the folded crease curves are ellipses, of which every second is a circle. As these crease-curves are not contained in parallel lines, this shape is not rigid-ruling foldable.

In a recent paper by [Mundilova et al. 23], the authors present two constructions to generate folded states of spirals using cones with planar creases; see Figure 6e.

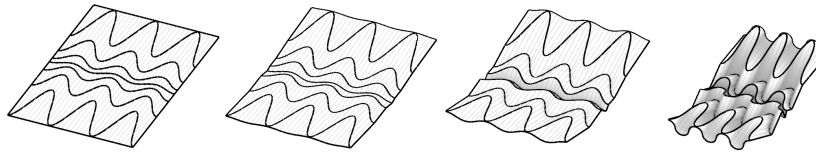

(a) *David Huffman's design using sine curves (undated) [Koschitz 14].*

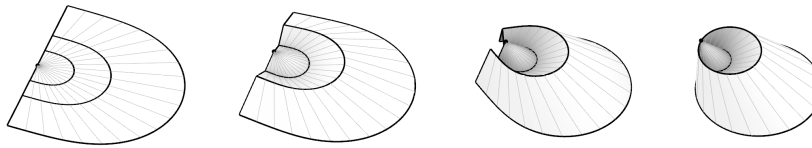

(b) *One half of Ron Resch's "Yellow Folded Cones: Kissing" (1969-1970) [Resch 23].*

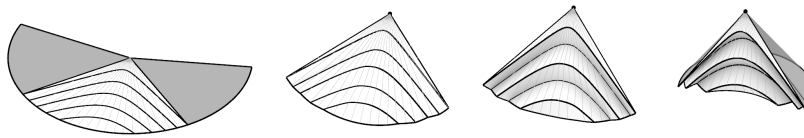

(c) *David Huffman's design of a right circular cone reflected along parallel planes that are also parallel to the cone's axis.*

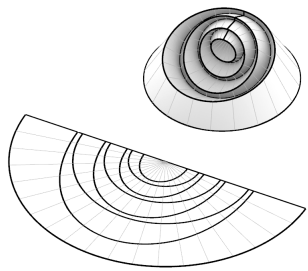

(d) *David Huffman's design of a right circular cylinder reflected seven times.*

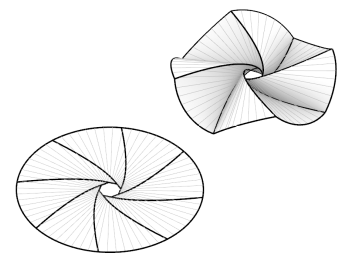

(e) *Origami spiral from cones with planar creases.*

Figure 6: *Illustrations of three origami designs with planar creases allowing a rigid-ruling folding motion.*

In both constructions, the planar creases are not in parallel planes. Consequently, even when adding a cut to the loop structure, this family of shapes (unless in the very special case that two creases are never connected by a ruling) is not rigid-ruling foldable.

5.3 Semi-discrete T-hedra

Let us now consider semi-discrete analogs of a special class of rigid-foldable quad surfaces called T-hedra (e.g. [Sauer 70]). By the refinement of a quad-strip, which keeps the planarity of the faces, the quads become the ruling of a developable strip in the limit [Pottmann et al. 08]. By doing this limiting process for all vertical strips of a T-hedron, we end up with semi-discrete surfaces composed of cylindrical surface patches, which are jointed along planar sections in accordance with Theorem 1. In the case of horizontal strips of a T-hedron we end up with semi-discrete surfaces composed of tangent-developble strips bounded by parallel planar curves, which also fits with Theorem 1. For more details on these isometric deformable semi-discrete surfaces including information on their rapid prototyping, we refer to [Maleczek et al. 22].

Finally, it should be mentioned that Theorem 1 also implies the non-existence of non-translational semi-discrete zip rows for a T-hedral zipper coupling, which was one of the open problems stated in [Sharifmoghaddam et al. 23]. For more details please see the referred paper.

6 Discretizations

Finally, we discuss discretizations that support this rigid-ruling compatibility between creases, such as the follow-up paper by [Demaine et al. 22] for the case of compatible constant angle creases presented in [Demaine et al. 18].

First, we consider the *circumscribed discretization*. In this approach, tangent planes are sampled, and pairs of adjacent tangent planes are intersected to obtain the discrete rulings. This method trivially preserves the property that the sampled tangents are either parallel or, in the case of a cylinder, have uniformly scaled slopes, making it a discretization that is rigidly foldable.

On the other hand, the *inscribed discretization* involves sampling the rulings and connecting them with planes. This method is applicable for cylinders and cones, as well as for their associated parallel, or in case of a cylinder, scaled crease curves. However, when sampling general developables, the rulings will not be coplanar, potentially necessitating a construction from a cone in these instances.

Finally, note that in the discrete case, an additional pair of polylines exists on some particular cones (caps of Bricard octahedron of the plane-symmetric type) allowing an isometric deformation that preserves their planarity [Nawratil 23]. This isolated solution, however, does not arise in the smooth case.

7 Conclusions and Future Work

Building upon the characterization of rigid-ruling folding compatible constant angle creases by [Demaine et al. 18], we have provided a characterization of rigid-ruling folding compatible planar creases, illustrated our theoretical findings with examples, and reviewed possible discretization strategies.

In future work, we plan to investigate other rigid-ruling-compatible crease combinations, such as those combining planar and constant angle creases.

Acknowledgement

The authors would like to thank the participants of the "Structural Origami Gathering 2023", particularly Tomohiro Tachi and Rupert Maleczek, for fruitful discussions and a collaborative atmosphere.

Georg Nawratil is supported by grant F77 (SFB "Advanced Computational Design") of the Austrian Science Fund FWF.

References

[Demaine et al. 11] Erik D. Demaine, Martin L. Demaine, and Duks Koschitz. "Reconstructing David Huffman's legacy in curved-crease folding." In *Origami*^{5}*: Proceedings of the 5th International Meeting on Origami in Science, Mathematics and Education (OSME 2011)*, pp. 39–52, 2011.

[Demaine et al. 15] Erik D. Demaine, Martin L. Demaine, David A. Huffman, Duks Koschitz, and Tomohiro Tachi. "Characterization of curved creases and rulings: Design and analysis of lens tessellations." In *Origami*^{6}*: Proceedings of the 6th International Meeting on Origami in Science, Mathematics and Education (OSME 2015)*, pp. 209–230, 2015.

[Demaine et al. 18] Erik D. Demaine, Martin L. Demaine, David A. Huffman, Duks Koschitz, and Tomohiro Tachi. "Conic crease patterns with reflecting rule lines." In *Origami*^{7}*: Proceedings of the 7th International Meeting on Origami in Science, Mathematics and Education (OSME 2018)*, pp. 573–590, 2018.

[Demaine et al. 22] Erik D. Demaine, Klara Mundilova, and Tomohiro Tachi. "Locally Flat and Rigidly Foldable Discretizations of Conic Crease Patterns with Reflecting Rule Lines." In *ICGG 2022-Proceedings of the 20th International Conference on Geometry and Graphics*, pp. 185–196. Springer, 2022.

[Jiang et al. 20] Caigui Jiang, Cheng Wang, Florian Rist, Johannes Wallner, and Helmut Pottmann. "Quad-Mesh Based Isometric Mappings and Developable Surfaces." *ACM Trans. Graph.* 39:4. doi:10.1145/3386569.3392430. Available online (https://doi.org/10.1145/3386569.3392430).

[Koschitz 14] Duks Koschitz. "Computational design with curved creases: David Huffman's approach to paperfolding." Ph.D. thesis, Massachusetts Institute of Technology, 2014.

[Liu et al. 06] Yang Liu, Helmut Pottmann, Johannes Wallner, Yong-Liang Yang, and Wenping Wang. "Geometric modeling with conical meshes and developable surfaces." In *ACM SIGGRAPH 2006 Papers*, pp. 681–689, 2006.

[Maleczek et al. 22] Rupert Maleczek, Kiumars Sharifmoghaddam, and Georg Nawratil. "Rapid prototyping for non-developable discrete and semi-discrete surfaces with an overconstrained mobility." In *Proceedings of the IASS Annual Symposium 2022 and the 13th Asian-Pacific Conference on Shell and Spatial Structures*, pp. 2302–2313. International Association for Shell and Spatial Structures (IASS), 2022.

[Mitani and Igarashi 11] Jun Mitani and Takeo Igarashi. "Interactive design of planar curved folding by reflection." In *Pacific Graphics Short Papers*, 2011.

[Mitani 12] Jun Mitani. "Column-shaped origami design based on mirror reflections." *Journal for Geometry and Graphics* 16:2 (2012), 185–194.

[Mundilova et al. 23] Klara Mundilova, Erik D. Demaine, Robert Lang, and Tomohiro Tachi. "Curved-Crease Origami Spirals Constructed from Reflected Cones." In *Proceedings of Bridges 2023: Mathematics, Art, Music, Architecture, Education, Culture*, 2023.

[Mundilova 23] Klara Mundilova. "Gluing and Creasing Paper along Curves: Computational Methods for Analysis and Design." Ph.D. thesis, Massachusetts Institute of Technology, 2023.

[Nawratil 23] Georg Nawratil. "Isometrically Deformable Cones and Cylinders Carrying Planar Curves." In *IFToMM World Congress on Mechanism and Machine Science*, pp. 218–227. Springer, 2023.

[Pottmann and Wallner 10] Helmut Pottmann and Johannes Wallner. *Computational Line Geometry*. Mathematics and Visualization, Springer Berlin Heidelberg, 2010.

[Pottmann et al. 08] Helmut Pottmann, Alexander Schiftner, Pengbo Bo, Heinz Schmiedhofer, Wenping Wang, Niccolo Baldassini, and Johannes Wallner. "Freeform surfaces from single curved panels." *ACM Transactions on Graphics (TOG)* 27:3 (2008), 1–10.

[Resch 23] Ron Resch, 2023. http://www.ronresch.org/.

[Sauer 70] Robert Sauer. *Differenzengeometrie*. Springer, 1970.

[Sharifmoghaddam et al. 23] Kiumars Sharifmoghaddam, Rupert Maleczek, and Georg Nawratil. "Generalizing rigid-foldable tubular structures of T-hedral type." *Mechanics Research Communications*, p. 104151.

[Tachi and Epps 11] Tomohiro Tachi and Gregory Epps. "Designing One-DOF mechanisms for architecture by rationalizing curved folding." In *International Symposium on Algorithmic Design for Architecture and Urban Design (ALGODE-AIJ)*, 5, 5, p. 6, 2011.

[Tachi 11] Tomohiro Tachi. "One-DOF rigid foldable structures from space curves." In *Proceedings of the IABSE-IASS Symposium*, pp. 20–23, 2011.

Klara Mundilova
klaramundilova.com, e-mail: klara.mundilova@gmail.com

Georg Nawratil
Institute of Discrete Mathematics and Geometry & Center for Geometry and Computational Design, TU Wien, Wiedner Hauptstraße 8-10/104, e-mail: nawratil@geometrie.tuwien.ac.at

A Proofs of Section 3

Proof of Lemma 1. First, let $\mathbf{S}_c(t,u) = \mathbf{C}(t) + u\mathbf{R}(t)$ be an isometric deformation of $\mathbf{s}_c(t,u)$ and $s_c'(t) = |\mathbf{c}'(t)| = |\mathbf{C}'(t)|$. By comparing the first fundamental forms of the two surfaces, we conclude that $|\mathbf{R}'(t)|^2 = |\mathbf{r}'(t)|^2$. Consequently, it follows that the first fundamental forms of $\mathbf{S}_\triangle(t,u) = u\mathbf{R}(t)$ and $\mathbf{s}_\triangle(t,u) = u\mathbf{r}(t)$ are identical. Therefore, the considered cones are isometric.

Conversely, let $\mathbf{S}_\triangle(t,u)$ be an isometric deformation of $\mathbf{s}_\triangle(t,u)$ and $s_c'(t) > 0$ some C^0 function. Up to Euclidean motion, we obtain a tangent developable surface by defining $\mathbf{C}(t)$ such that $\mathbf{C}'(t) = s_c'(t)\mathbf{R}(t)$ and setting $\mathbf{S}_c(t,u) = \mathbf{C}(t) + u\mathbf{R}(t)$. To show that $\mathbf{s}_c(t,u)$ and $\mathbf{S}_c(t,u)$ are isometric, we again compare their first fundamental forms. It follows from the comparison of the first fundamental forms of $\mathbf{s}_\triangle(t,u)$ and $\mathbf{S}_\triangle(t,u)$ that $|\mathbf{R}'(t)|^2 = |\mathbf{r}'(t)|^2$, which implies that the first fundamental forms of $\mathbf{s}_c(t,u)$ and $\mathbf{S}_c(t,u)$ are the same. □

Proof of Lemma 2. To prove this claim, we compute

$$\mathbf{X}_c'(t) = \big(s_c'(t) + l'(t)\big)\,\mathbf{R}(t) + l(t)\mathbf{R}'(t) \quad \text{and} \quad \mathbf{X}_\triangle'(t) = l_\triangle'(t)\mathbf{R}(t) + l_\triangle(t)\mathbf{R}'(t).$$

It follows from Equation (10) (left) that

$$\big|\mathbf{X}_c'(t) \times \mathbf{X}_\triangle'(t)\big| = \big|\big((s_c'(t) + l'(t))l_\triangle(t) - l(t)l_\triangle'(t)\big)\,\big(\mathbf{R}(t) \times \mathbf{R}'(t)\big)\big| = 0,$$

which implies the claim. □

B Proof of Theorem 1 in Section 4

In the following proof, we will use subscripts to denote the quantities corresponding to the first and second surfaces, and lower and uppercase letters to denote their development or 3D configuration, respectively. Specifically, we will represent the common arc lengths of $\mathbf{x}_i(t)$ and $\mathbf{X}_i(t)$ as $s_i(t)$, the curvatures of $\mathbf{x}_i(t)$ as $k_i(t)$, and the ruling angles as $\theta_i(t)$. Additionally, the curvatures of $\mathbf{X}_i(t)$ will be denoted by $K_i(t)$, with an acknowledgment that their torsions, $\tau_i(t)$, are zero. The inclination angles will be represented by $\varphi_i(t)$.

B.1 Step 1: Preparation

In the first step of this proof, we establish two constraints that are necessary for a valid configuration with two planar curves, and present the main idea of the proof.

Constraint 1: Compatibility in 2D. First, we derive a constraint that arises from the fact that the curves $\mathbf{x}_1(t)$ and $\mathbf{x}_2(t)$ are located on the same planar surface. For this purpose, we express the ruling vector in terms of both orthonormal frames $(\mathbf{t}_i(t), \mathbf{n}_i(t))$ of $\mathbf{x}_i(t)$, as

$$\mathbf{r}(t) = \cos\theta_i(t)\;\mathbf{t}_i(t) + \sin\theta_i(t)\;\mathbf{n}_i(t).$$

Using Equation (8), the first derivative of the ruling reads

$$\mathbf{r}'(t) = \left(\mathbf{s}_i'(t)k_i(t) + \theta_i'(t)\right)\left(-\sin\theta_i(t)\ \mathbf{t}_i(t) + \cos\theta_i(t)\ \mathbf{n}_i(t)\right).$$

Since the absolute values of the ruling vector w.r.t. either frame are the same, it follows that

$$s_1'(t)k_1(t) + \theta_1'(t) = s_2'(t)k_2(t) + \theta_2'(t). \tag{12}$$

Constraint 2: Compatibility in 3D. To ensure that the resulting isometric deformations correspond to the same 3D surface, we require the ruling curvatures (see Equation (9)) to be identical, which yields the following relation under consideration of Equation (7),

$$V_1(t) = \frac{s_1'(t)k_1(t)}{\sin\theta_1(t)}\tan\varphi_1(t) = \frac{s_2'(t)k_2(t)}{\sin\theta_2(t)}\tan\varphi_2(t) = V_2(t). \tag{13}$$

When isometrically deforming the developable patches $\mathbf{s}_1(t,u)$ and $\mathbf{s}_2(t,u)$ such that their directrices remain planar, it follows from Equation (11), that the inclination angles of the isometric deformations $\mathbf{S}_i(t,u)$ can be written as

$$\varphi_i(t) = \arcsin\left(c_i e^{I_i(t)}\right) \qquad \text{for} \qquad I_i(t) = \int_0^t s_i'(\tilde{t})k_i(\tilde{t})\cot\theta_i(\tilde{t})\,d\tilde{t}, \tag{14}$$

where $|c_1| < c_{1,\max}$ and c_2 are appropriate constants.

Using the trigonometric equality $\tan(\arcsin(x)) = x(1-x^2)^{-\frac{1}{2}}$ for the inclination angles in Equation (14), Equation (13) can be rewritten as

$$F_1(t)\frac{c_1 e^{I_1(t)}}{\sqrt{1-c_1^2 e^{2I_1(t)}}} = F_2(t)\frac{c_2 e^{I_2(t)}}{\sqrt{1-c_2^2 e^{2I_2(t)}}}, \quad \text{with} \quad F_i(t) := \frac{s_i'(t)k_i(t)}{\sin\theta_i(t)}. \tag{15}$$

Main idea of proof. In the following, our goal is to deduce properties of the arc-lengths, curvatures, and ruling angles of the patches $\mathbf{s}_i(t,u)$ satisfying Equation (12), such that for all c_1 with $|c_1| < c_{1,\max}$, we can identify an appropriate constant $c_2(c_1)$ that satisfies Equation (15) for all t.

Remark. Note that tangent-parallel curves satisfy Equations (12) and (15) for $c_2(c_1) = c_1$, as in such cases $s_1'(t)k_1(t) = s_2'(t)k_2(t)$, $\theta_1(t) = \theta_2(t)$, and $\varphi_1(t) = \varphi_2(t)$.

B.2 Step 2: Analysis of Cylinders and Cones

In the following analysis, we first consider only parameter values t where $k_1(t) \neq 0$, which implies that $F_i(t) \neq 0$ and $I_i'(t) \neq 0$. Note that Equation (15) is trivially satisfied when $c_1 = c_2 = 0$, which corresponds to the planar configuration. We will therefore also exclude the case where $c_1 = 0$. Since $F_2(t) \neq 0$, Equation (15) implies that $c_2 \neq 0$.

We start our analysis for pairs of curves on planar developable patches that are initially not restricted to be cylinders or cones. Solving Equation (15) for the square of c_2 yields

$$c_2^2 = \frac{A(t)c_1^2}{B(t)c_1^2 + C(t)},$$

where

$$A(t) = F_1(t)^2 e^{2I_1(t)}, \quad B(t) = \left(F_1(t)^2 - F_2(t)^2\right) e^{2I_1(t)} e^{2I_2(t)}, \quad C(t) = F_2(t)^2 e^{2I_2(t)}.$$

As c_2 is constant in t, differentiation w.r.t. parameter t should be zero, that is,

$$0 = \frac{d}{dt} c_2^2 = \frac{\left(A'(t)B(t) - A(t)B'(t)\right) c_1^2 + A'(t)C(t) - A(t)C'(t)}{\left(B(t)c_1^2 + C(t)\right)^2} c_1^2.$$

This equation must be satisfied for all suitable values of c_1. Therefore, we require that the coefficients of c_1^4 and c_1^2 in the numerator vanish, leading to the following two constraints:

$$0 = A'(t)B(t) - A(t)B'(t) \qquad \text{and} \qquad 0 = A'(t)C(t) - A(t)C'(t). \tag{16}$$

Additionally, note that the denominator cannot vanish for all t, which is equivalent to $B(t) = C(t) = 0$, since our assumptions imply that $C(t) \neq 0$.

We simplify Equation (16) (right), which results in

$$0 = I_1'(t) - I_2'(t) + \frac{F_1'(t)}{F_1(t)} - \frac{F_2'(t)}{F_2(t)}.$$

Using integration, it follows that

$$0 = I_1(t) - I_2(t) + \ln F_1(t) - \ln F_2(t) + \text{const},$$

which simplifies to

$$\frac{F_1(t)}{F_2(t)} = c_3 \frac{e^{I_2(t)}}{e^{I_1(t)}}, \tag{17}$$

where $c_3 \neq 0$ is a constant. Note that the constant c_3 only depends on $F_i(t)$ and $I_i(t)$, thus only on the geometry, and is independent of c_1 or c_2.

Next, we consider the equation which results from adding $e^{2I_1(t)}$ times the right equation of Equation (16) to its left one:

$$A'(t)\left(B(t) + e^{2I_1(t)}C(t)\right) - A(t)\left(B'(t) + e^{2I_1(t)}C'(t)\right) = 0.$$

Simplifications of this equation result in

$$\frac{F_1(t)^2}{F_2(t)^2} = \frac{I_1'(t)}{I_2'(t)}. \tag{18}$$

Combining Equation (17) with Equation (18) yields

$$I_1'(t)e^{2I_1(t)} = c_3^2 I_2'(t)e^{2I_2(t)}. \tag{19}$$

We proceed by applying Equations (12), (17), and (19), as constraints to pairs of curves on cylinders and cones.

B.2.1 Isometric Deformation of a Cylinder

First, we consider two parametrizations of the same cylinder, $\mathbf{s}_i(t,u) = \mathbf{x}_i(t) + u\mathbf{r}(t)$, where

$$\mathbf{x}_i(t) = (t,0) + l_i(t)\mathbf{r}(t) \qquad \text{and} \qquad \mathbf{r}(t) = (0,1),$$

where $l_i(t)$ are two initially unknown C^2 length function.

Using the descriptions in Section 2.2, we compute the following quantities

$$s_i'(t)k_i(t) = \frac{l_i''(t)}{1+l_i'(t)^2} \qquad \text{and} \qquad \theta_i(t) = \arccos\left(\frac{l_i'(t)}{\sqrt{1+l_i'(t)^2}}\right),$$

which simplify the expressions in Equation (14) to

$$I_i(t) = \frac{1}{2}\log\left(1+l_i'(t)^2\right) \qquad \text{and} \qquad e^{I_i(t)} = \sqrt{1+l_i'(t)^2}. \tag{20}$$

This yields the inclination angle

$$\varphi_i(t) = \arcsin\left(c_i\sqrt{1+l_i'(t)^2}\right),$$

for constants c_1 and $c_2(c_1)$ such that $|c_1| \le c_{1,\max}$.

Since in the case of cylinders, $|\mathbf{r}'(t)| = 0$, Equation (12) is trivially satisfied. Additionally, Equations (17) and (19) simplify to

$$l_1''(t) = c_3 l_2''(t) \qquad \text{and} \qquad l_1'(t)l_1''(t) = c_3^2 l_2'(t)l_2''(t).$$

Since $l_1''(t) = 0$ if and only if $l_2''(t) = 0$, there are two possible scenarios:

- If $l_i''(t) \neq 0$, then $l_1'(t) = c_3 l_2'(t)$ and $l_1(t) = c_3 l_2(t) + c_4$. This case corresponds to pairs of curves lying in planes whose normals are coplanar with the ruling directions, as discussed by [Nawratil 23]. Inserting this into Equation (15) yields the following connection between the constants:

$$c_2^2 = \frac{c_1^2 c_3^2}{1+c_1^2(c_3^2-1)} \qquad \text{where} \qquad c_2 < \frac{c_{1,\max}^2 c_3^2}{1+c_{1,\max}^2(c_3^2-1)}.$$

- If $l_i''(t) = 0$, then $l_i(t) = a_i t + b_i$, and the curves are linear functions. Then Equation (15) is trivially satisfied for all pairs of constants $c_2 < c_{1,\max} = 1$.

B.2.2 Isometric Deformation of a Cone

Next, we consider two parametrizations of the same cone, $\mathbf{s}_i(t,u) = \mathbf{x}_i(t) + u\mathbf{r}(t)$, with

$$\mathbf{x}_i(t) = \mathbf{v} + l_i(t)\mathbf{r}(t) \qquad \text{and} \qquad \mathbf{r}(t) = (\cos t, \sin t),$$

where $\mathbf{v}$ is the cone apex and $l_i(t)$ are two initially unknown C^2 length functions.

Similarly to the cylinder case, we use the description in Section 2.2 to compute the quantities

$$s_i'(t)k_i(t) = \frac{l_i(t)^2 + 2l_i'(t)^2 - l_i(t)l_i''(t)}{l_i(t)^2 + l_i'(t)^2} \quad \text{and} \quad \theta_i(t) = \arccos\left(\frac{l_i'(t)}{\sqrt{l_i(t)^2 + l_i'(t)^2}}\right),$$

which simplify the expressions in Equation (14) to

$$I_i(t) = 2\log l_i(t) - \frac{1}{2}\log\left(l_i(t)^2 + l_i'(t)^2\right) \quad \text{and} \quad e^{I_i(t)} = \frac{l_i(t)^2}{\sqrt{l_i(t)^2 + l_i'(t)^2}}.$$

This yields the inclination angle

$$\varphi_i(t) = \arcsin\left(c_i \frac{l_i(t)}{\sqrt{l_i(t)^2 + l'(t)^2}}\right),$$

for a constants c_1 and $c_2(c_1)$ such that $|c_1| \leq c_{1,\max}$.

It follows that inserting into Equation (12) simplifies to

$$\frac{l_1(t)^2 + 3l_1'(t)^2 - 2l_1(t)l_1''(t)}{l_1(t)^2 + l_1'(t)^2} = \frac{l_2(t)^2 + 3l_2'(t)^2 - 2l_2(t)l_2''(t)}{l_2(t)^2 + l_2'(t)^2},$$

and Equation (17) yields

$$\frac{l_1(t)\left(l_1(t)^2 + 2l_1'(t)^2 - l_1(t)l_1''(t)\right)}{l_1(t)^2 + l_1'(t)^2} = c_3 \frac{l_2(t)\left(l_2(t)^2 + 2l_2'(t)^2 - l_2(t)l_2''(t)\right)}{l_2(t)^2 + l_2'(t)^2}.$$

Since $l_1(t)^2 + 2l_1'(t)^2 - l_1(t)l_1''(t) = 0$ if and only if $l_2(t)^2 + 2l_2'(t)^2 - l_2(t)l_2''(t)$, we distinguish between two scenarios:

- If $l_i(t)^2 + 2l_i'(t)^2 - l_i(t)l_i''(t) \neq 0$, we solve the two equations above for $l_1''(t)$ and $l_2''(t)$. When setting each pair of expressions for $l_i''(t)$ simplify to

$$\frac{(l_1(t) - c_3 l_2(t))\left(l_i(t)^2 + l_i'(t)^2\right)\left(l_j(t)^2 + 2l_j'(t)^2 - l_j(t)l_j''(t)\right)}{l_i(t)\left(l_j(t)^2 + l_j'(t)^2\right)} = 0.$$

  It follows that $l_1(t) = c_3 l_2(t)$, which corresponds to pairs of scaled curves with respect to the apex, having parallel tangents. This solution satisfies also Equation (19). In this case, Equation (15) yields the following connection between the constants:

$$c_2^2 = c_1^2 c_3^2 \qquad \text{where} \qquad c_2 < c_{1,\max}.$$

- If $l_i(t)^2 + 2l_i'(t)^2 - l_i(t)l_i''(t) = 0$, it follows that the solution reads

$$l_i(t) = \frac{a_i}{\cos(t + b_i)},$$

for some constants a_i and b_i corresponding to straight lines on the cone (in polar parametrization). It can be verified that this solution again satisfies also Equation (19). Furthermore, Equation (15) is again trivially satisfied for all pairs of constants c_1 and c_2 with $c_2 < c_{1,\max} = 1$.

B.3 Step 3: Considerations for Isolated Values with Vanishing Curvature

We now consider a $\mathbf{x}_1(t)$ on a cylinder or a cones with isolated parameter values $T^* = \{t_1^*, t_2^*, \ldots, t_m^*\}$ for $t_j^* \in (t_{\min}, t_{\max})$ where $k_1(t_j^*) = 0$.

In both the cylinder and cone case, we first consider a non-empty interval T' with $k_1(t) \neq 0$ for all $t \in T'$. For a configuration that maintains the planarity of $\mathbf{x}_1(t)$, let $\mathbf{x}_2(t)$ be a curve that remains planar during all isometric deformations preserving the planarity of $\mathbf{x}_1(t)$. Let E_i denote its base plane of $\mathbf{X}_i(t)$.

For $t \in T \backslash T'$, as we are only considering planar curves, the only admissible parts of the remaining second curve coincide with the intersection of the 3D configurations of the developable patch with E_2:

- In case of a cylinder, this intersection is well-defined and the remaining points of the curve still satisfy the characteristic that the normal of E_2, the normal of E_1, and the ruling direction are coplanar.
- In case of a cone, E_2 and E_1 are parallel. Consequently, if the configuration is bend and the planes did not contain the cone apex for $t \in T'$, they will not do so for $t \in T$. Consequently, the intersection is again well-defined and the extension satisfies the characteristic property that the base planes are parallel.

In both cases, $s_1'(t_j^*)k_1(t_j^*) = 0$ implies $s_2'(t_j^*)k_2(t_j^*) = 0$, hence also for parameter values $t_j^* \in T^*$, the necessary conditions in Equation (12) and Equation (13) are satisfied.

B.4 Step 4: Isometric Deformations of Tangent Developables from Cones

In the following, we argue that if $\mathbf{s}(t,u)$ is a developable patch with $|\mathbf{R}'(t)| \neq 0$, except at isolated points, then the only curvature-continuous curves that remain planar during isometric deformations (which preserve the planarity of the directrix) are those that are tangent-parallel to the directrix.

Our argument first considers an interval $T' \subset T$ with $|\mathbf{R}'(t)| \neq 0$ for all $t \in T'$. In this context, we represent the considered developable patch in terms of a (possibly singular) edge of regression, which does not contain a point at infinity. We will now use the findings from Section 3.1 to demonstrate our claim by contradiction.

Suppose there exists a developable patch with $|\mathbf{R}'(t)| \neq 0$, except at isolated points, that allows for an isometric deformation such that two curves, $\mathbf{x}_1(t)$ and $\mathbf{x}_2(t)$, which are neither straight nor tangent-parallel, remain planar. Since the curves are not tangent-parallel, their carrier planes would not be parallel. In this case, we could examine the corresponding curves on a the ruling cone. Since any isometric deformation of the tangent developable surface would result in an isometric deformation of a cone (as shown in Lemma 1), we would have the configuration

of the curves $\mathbf{X}_{1,\triangle}(t)$ and $\mathbf{X}_{2,\triangle}(t)$. According to Lemma 2, the tangents of these curves would be parallel to the tangents of the corresponding curves $\mathbf{X}_1(t)$ and $\mathbf{X}_2(t)$. Thus, they would lie in two planes, which, by assumption, were not parallel. This would lead to a contradiction.

Similar to the previous discussion, for isolated parameter values where $|\mathbf{R}'(t)| = 0$, the above argument cannot be applied. However, if $\mathbf{X}_2(t)$ is an appropriate second curve for all $t \in T'$, its extension must reside in the intersection of the base plane of $\mathbf{X}_2(t)$ and the considered surface configuration. Upon the existence of such a (curvature continuous) extension, this results in a tangent-parallel curve for all $t \in T$.